Dynamic electric field alignment of metal-organic framework microrods

Fei Cheng[†,a] Adam J. Young[†,ab] Jean-Sebastien G. Bouillard,[c] Neil T. Kemp,[c] Rémy Guillet-Nicolas,[d] Connor H. Hall,[c] David Roberts,[a] Ayoub H. Jaafar,[c] Ali M. Adawi,[c] Freddy Kleitz,[d] Arnout Imhof,[e] Michael R. Reithofer,*[b] Jia Min Chin*[ab]

a. Department of Chemistry, University of Hull, Hull, UK

b. Institute of Inorganic Chemistry, University of Vienna, Faculty of Chemistry, Vienna, Austria

c. Department of Physics and Mathematics, University of Hull, Hull, UK

d. Faculty of Chemistry, Department of Inorganic Chemistry – Functional Materials, University of Vienna, Vienna, Austria

e. Soft Condensed Matter & Biophysics, Debye Institute for Nanomaterials Science, Utrecht University, Utrecht, The Netherlands

Supporting Information

Table of Contents

Materials and Methods

Trimethoxy(octadecyl)silane (TMODS, 90%), butylamine (99.5%), chlorocyclohexane (99%) and bromobenzene (99.5%) were sourced from Sigma-Aldrich. Hollow rectangle capillaries (ID 0.05 x 1.00 mm, length: 50 mm, wall thickness: 0.05 mm) and square capillaries (ID 0.20 x 0.20 mm, length: 50 mm, wall thickness: 0.1 mm) were purchased from VitroCom. Norland 68 Optical Adhesive was obtained from TechOptics, UK. NU-1000 was synthesized according to previously reported literature procedures.[1] Inductively coupled plasma – mass spectrometry showed NU-1000 to contain: Zr 22.13%.

Modification of NU-1000: NU-1000 (30 mg), which has been dried at 100 °C overnight, was added in a glass sample tube. Then, 450 mg of a solution of TMOS, butylamine and dried toluene (1/1/10, v/v/v) was added to the sample tube. The suspension mixture was sonicated for 4 h. The colloidal rods were then centrifuged and washed with toluene and cyclohexane. The obtained micro rods were dried under vacuum at 30 °C overnight. Inductively coupled plasma – mass spectrometry showed the resulting NU-1000_{Si} to contain: Zr 13.98% and Si 5.98%.

Preparation of NU-1000_{Si} suspension in bromobenzene (using the example of a 0.1% suspension): Bromobenzene (0.865 mL) was added to a sample tube containing NU-1000_{Si} (1.29 mg). The mixture was then probe sonicated (Vibra-CellTM ultrasonic processor, VC 100, Sonics & Materials INC) for one minute, twice, to give a homogenous stable (0.1%) suspension.

Preparation of sample cell: The sample cell construct is shown in Figure 2a.

Opposite facing sides of the hollow rectangle capillary surface were externally coated first with chromium (3 nm), then gold (7 nm) by e-beam deposition with a HHV Lab coater Auto 500. To fill the Cr/Au coated capillary cell, one end was dipped in a suspension of NU-1000_{Si} in solvent (0.25 wt%) to fill the suspension into the cell via capillary action. Both sides of the capillary were then sealed with UV-glue Norland 68. The capillary was set on the two 55 µm silver wires which were wrapped around a glass slide. One of the silver wires was connected with a standard electronic wire and served as an electrical contact. Another electrical contact was made by sticking a silver wire on another Cr/Au coated surface with silver paint and then connected with standard electronic wire. The wires were attached to a wave function generator (WaveTek 95 Arbitrary Function Generator) coupled to an oscilloscope (Tektronix TDS2024C) for controlling the applied AC electric field.

Electrooptical Measurements:

Electrooptical measurements were carried out using the glass capillary cells described above. The cell was studied using a polarized optical microscope (Olympus BX51) equipped with a photodetector (Thorlabs PDA100A - Si Switchable Gain Detector) coupled to an oscilloscope (Tektronix TDS2024C) for voltage gain measurements.

Confocal microscopy measurement: Confocal imaging was performed using a Zeiss LSM710 Laser Scanning Confocal Microscope, x40 and x63 C-Apochromat NA 1.3 WD 280 mm oil objective. Fluorescence was acquired in 420-480 nm range and excited with 405 nm UV laser.

Physisorption measurements:

N_2 adsorption/desorption isotherm measurements at -196 °C were performed using an AutosorbiQ2-MP sorption instrument (Quantachrome Instruments, Anton Paar, Boynton Beach, FL, USA). Prior to the measurements, samples were outgassed under vacuum at 150 °C for 12 h. Apparent BET specific surface area, S_{BET}, was determined via the Brunauer Emmett-Teller (BET) equation from adsorption data obtained at P/P_0 between 0.05 and 0.2. Relevant pore size distribution was obtained from the adsorption branch of the isotherms by applying the kernel of (metastable) Non-Local Density Functional Theory (NLDFT) adsorption isotherms, considering a polar surface and a cylindrical pore model,[2] which is currently the most accurate kernel for such MOF materials, since Quenched Solid Density Functional Theory (QSDFT) kernels are not yet commercially available for oxidic/silica surfaces.[3] NLDFT micropore and total pore volumes were determined using the same kernel. The calculations were carried out using the ASiQWin software 5.0 provided by Quantachrome Instruments.

Thermogravimetric analysis:

Thermogravimetric analyses (TGA) were performed using a Netzsch STA 449-F3 Jupiter analyzer, from room temperature to 800 °C with a heating rate of 10 °C·min^{-1} with an isothermal segment of 30 min at 100 °C. A nitrogen flow of 20 mL·min^{-1} as well as an additional protective nitrogen flow of 20 mL·min^{-1} were used. The percentage of burnt species was calculated based on the detected mass loss between 100 and 800 °C.

SEM images:

SEM images were captured on a Zeiss Supra 55 VP electron microscope. All samples were gold sputter coated prior to analysis, with the exception of samples utilized for SEM-EDX measurements.

Polarization measurements:

A continuous wave laser diode, with an emission wavelength of 405 nm, was used to illuminate the MOF solution at normal incidence. The intensity of the irradiation was controlled using a variable neutral density filter, and the polarisation orientation was controlled using a linear polariser followed by a half wave plate. The resulting MOF fluorescence was collected in transmission by a Mitutoyo Plan Apo infinity corrected long working distance objective lens (magnification 10x, NA 0.28) before being injected into a 200 μm diameter optical fibre coupled spectrometer (Avantes-ULS3648 Spectrometer). A long-pass filter (cut-off wavelength 437 nm) was used to remove the laser excitation from the MOF fluorescence signal. The polarisation of the incident light was rotated in 10˚ increment between each measurement, and the fluorescence spectra were taken with a 5-second integration time at a constant power and position on the sample. The samples were measured with and without applied voltage to determine the MOF alignment under applied electric field.

Inductively coupled plasma-mass spectrometry (ICP-MS):

The sample was weighed into a Teflon digestion vessel (CEM XP1500) and 3 mL nitric acid (Romil SpA trace metal grade) and 0.1 mL HF (Romil SpA grade) were added. After digested in microwave (CEM MARS system), the digest was diluted with Elga Purelab water by weight to about 23 g. Analysis for Zr and Si were performed on the Perkin Elmer Optima 5300DV emission ICP instrument. The emission wavelengths were 343.823 nm (Zr) and 251.611 nm (Si). The elements of interest were calibrated to 10 ppm and measurements in the digests were calculated to correspond to percentage by weight in the original dry solid powders.

Zeta potential measurements

Zeta potential measurements were carried out using a Malvern Zetasizer Nano ZS-series with a universal solvent resistant dip cell.

Figure S1. SEM images of NU-1000

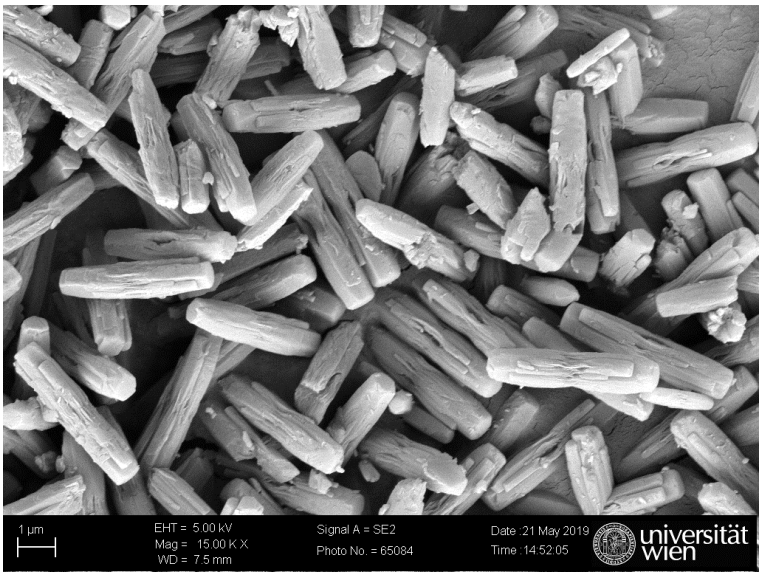

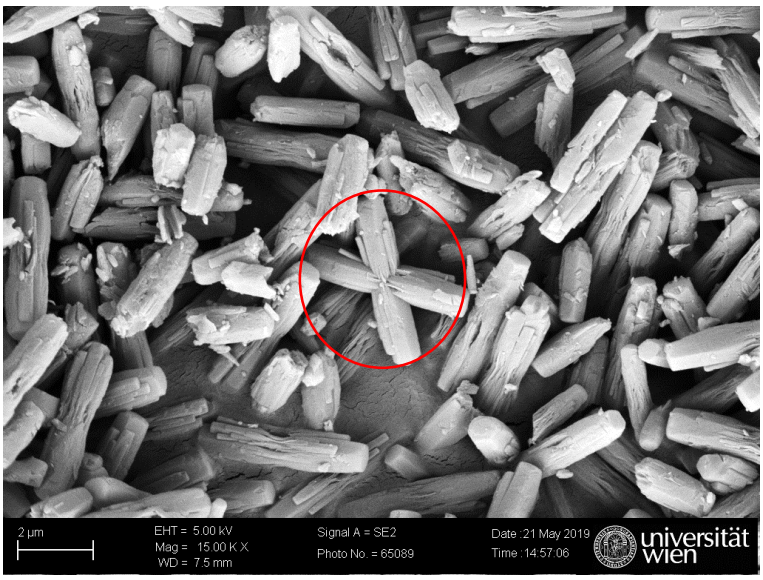

SEM image showing a cross-shaped NU-1000 particle, circled.

Figure S2. SEM images of NU-1000$_{Si}$

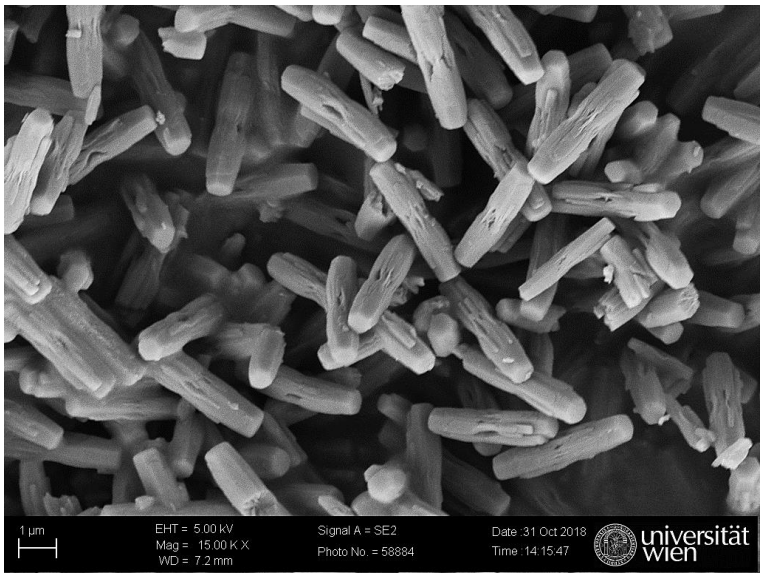

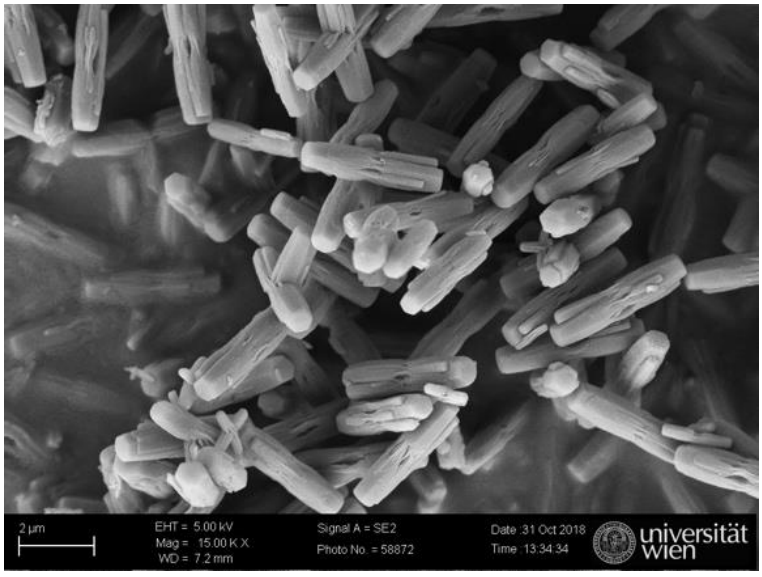

Figure S3. Photograph of NU-1000 (1) and NU-1000$_{Si}$ (2) dispersed in bromobenzene.

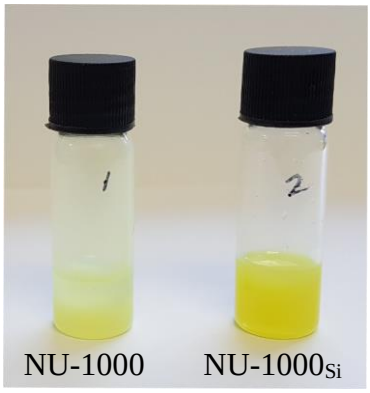

The unmodified NU-1000 sediments rapidly whereas NU-1000$_{Si}$ disperses more readily in bromobenzene and forms a stable suspension.

Figure S4. FTIR of NU-1000 and NU-1000$_{Si}$

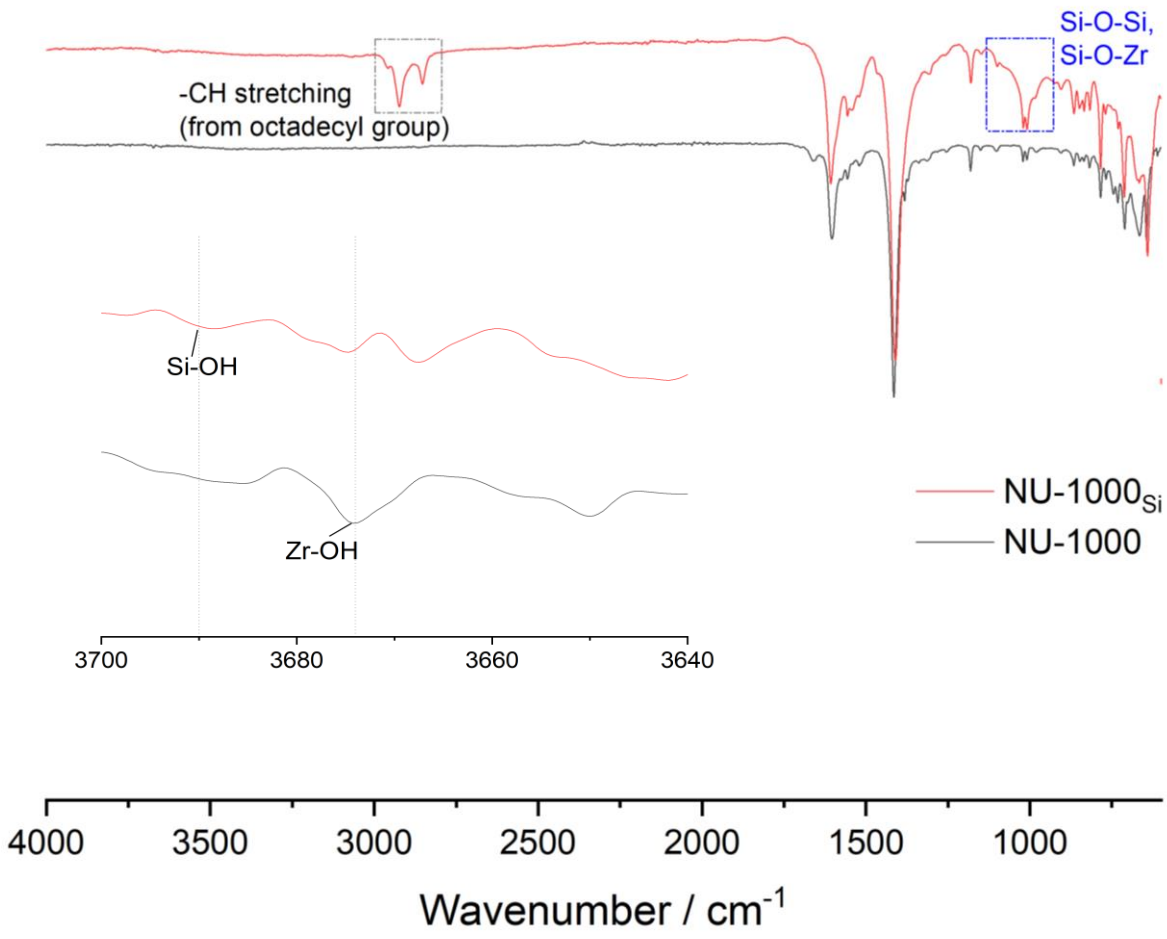

The peak at 3674 cm^{-1} NU-1000 (blue) can be assigned to terminal O−H stretches on the zirconia nodes.[4] After modification with trimethoxy(octadecyl)silane, the terminal O−H stretch has significantly attenuated and there are new stretches around 2966-2850 cm^{-1} due to C-H stretches from the octadecyl moiety. There also appears to be a new Si-OH stretch around 3688 cm^{-1} and a broad band from 1130 – 930 cm^{-1} attributable to overlapping stretches due to Si-O-Si and Si-O-Zr bonds.[5,6]

Figure S5. PXRD of NU-1000 and NU-1000$_{Si}$

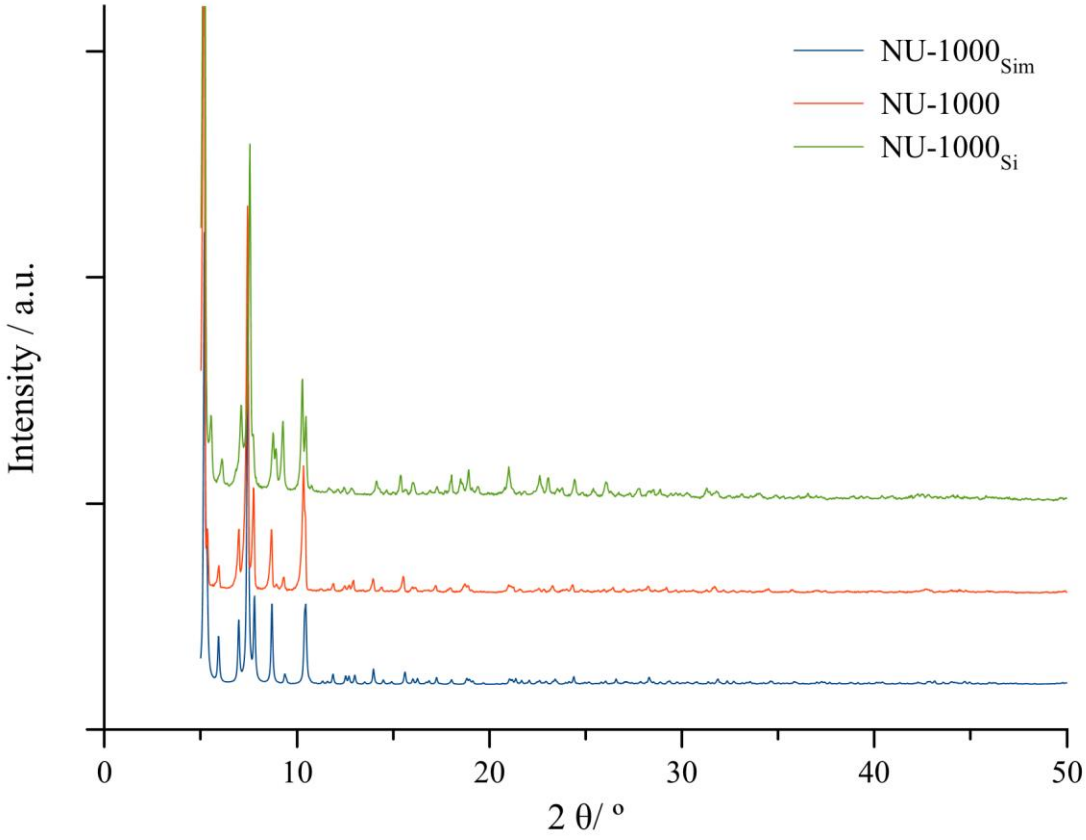

Figure S6. Confocal microscope images of NU-1000$_{Si}$ suspensions in bromobenzene

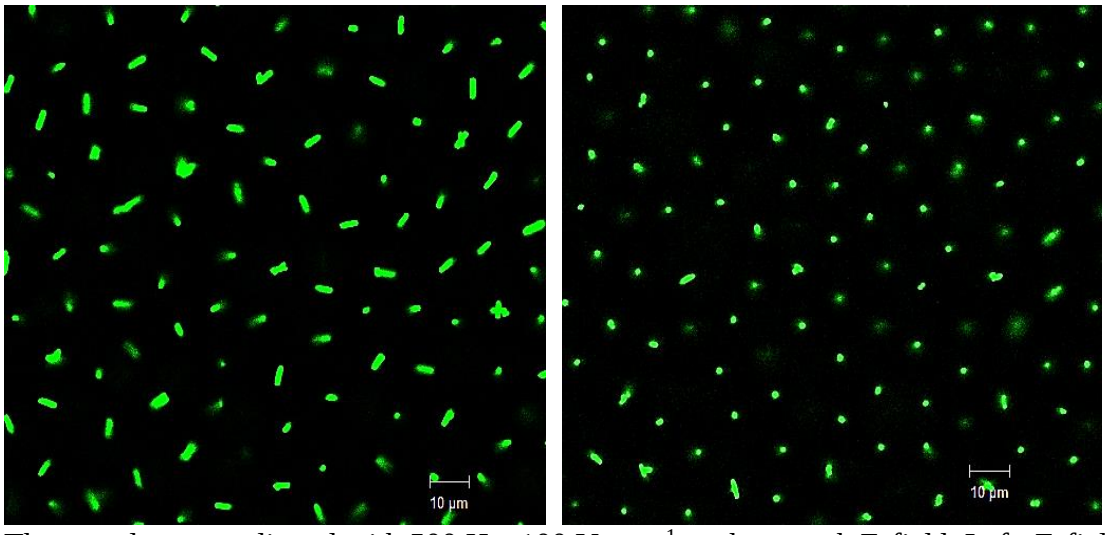

The samples were aligned with 500 Hz, 100 V·mm^{-1} peak-to-peak E-field. Left: E-field is OFF; Right: E-field is ON. The field direction is perpendicular to the plane of the image.

Figure S7. Plot of NU-1000$_{Si}$ alignment response time against A.C. field frequency

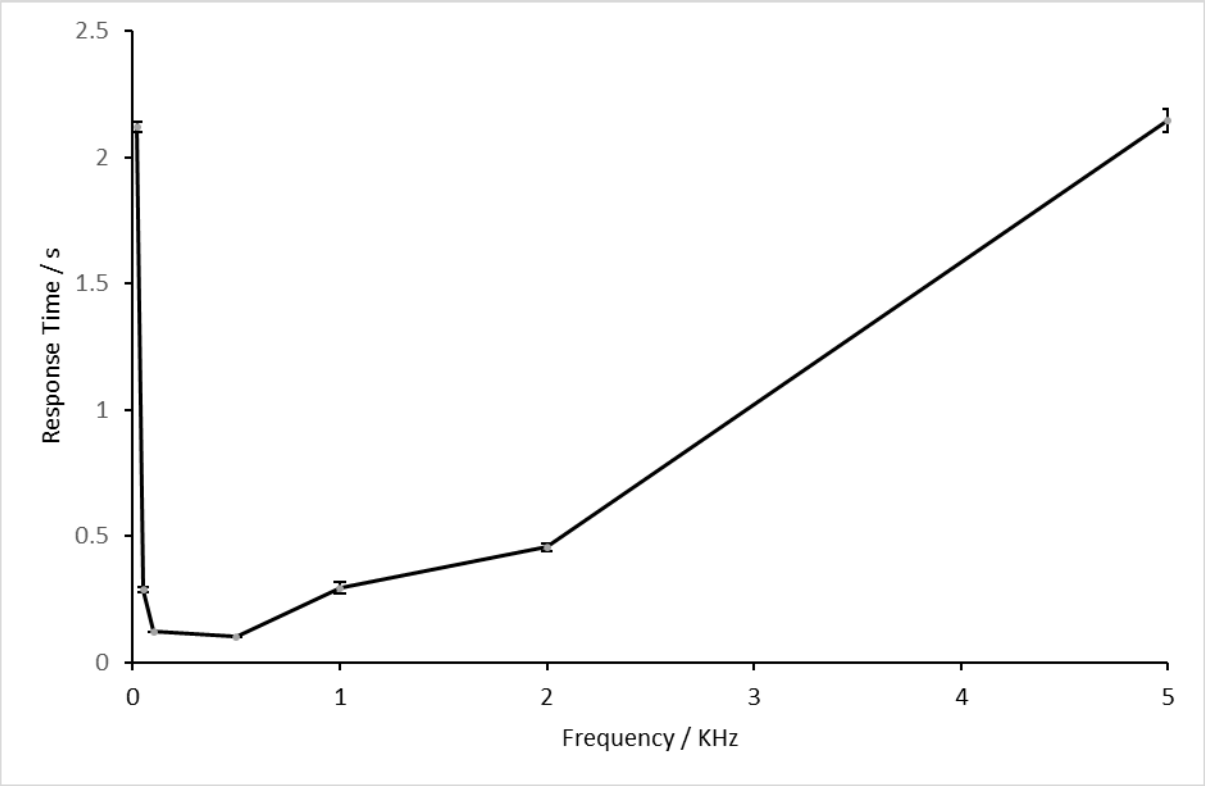

The alignment response of NU-1000$_{Si}$ decreases as the A.C. field frequency approaches 0 Hz and no alignment occurs under a static (D.C.) electric field. The absence of alignment under a D.C. electric field suggests the presence of a large screening effect caused by the formation of an electrical double layer at the electrode-solution interface. Under static electric field conditions, even in non-aqueous systems, ions present will migrate to oppositely charged electrodes to form the electrical double layer.[7-8] The NU-1000$_{Si}$ microrods are thus shielded from the E-field by these ions, and do not align under these conditions. This is further supported by the lack of observable electrophoretic motion of the microrods towards the electrodes under a static electric field. However, once the E-field frequency is increased such that the ions are unable to move with respect to the oscillating charges on the electrodes, the shielding effect diminishes and the NU-1000$_{Si}$ microrods respond to the E-field and align.

Table S1. Zeta potential measurements for NU-1000 and NU-1000$_{Si}$ in bromobenzene

Sample	Zeta potential (mV)
NU-1000 (0.05 mg·mL^{-1})	-76 ± 6
NU-1000$_{Si}$ (0.05 mg·mL^{-1})	- 69 ± 5

It should be noted that as the NU-1000 and NU-1000$_{Si}$ microrods are non-spherical, and the solvent is non-aqueous, that these measurements should only be taken as qualitative rather than quantitative indicators that the MOFs are negatively charged when dispersed in bromobenzene.

Figure S8. N_2 adsorption (open circles)-desorption (solid triangles) isotherms (-196 °C) for NU-1000 and NU-1000_{Si}

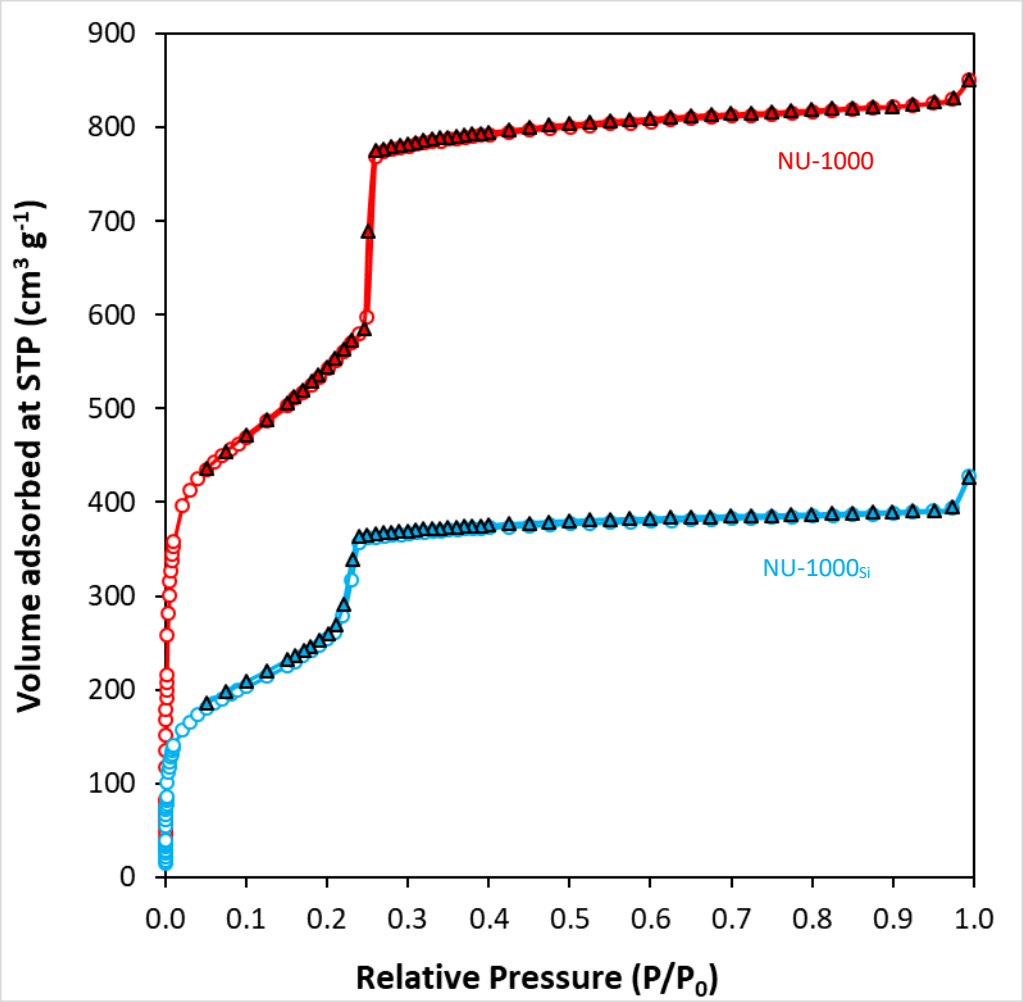

Figure S9. NLDFT pore size distribution of NU-1000 and NU-1000$_{Si}$

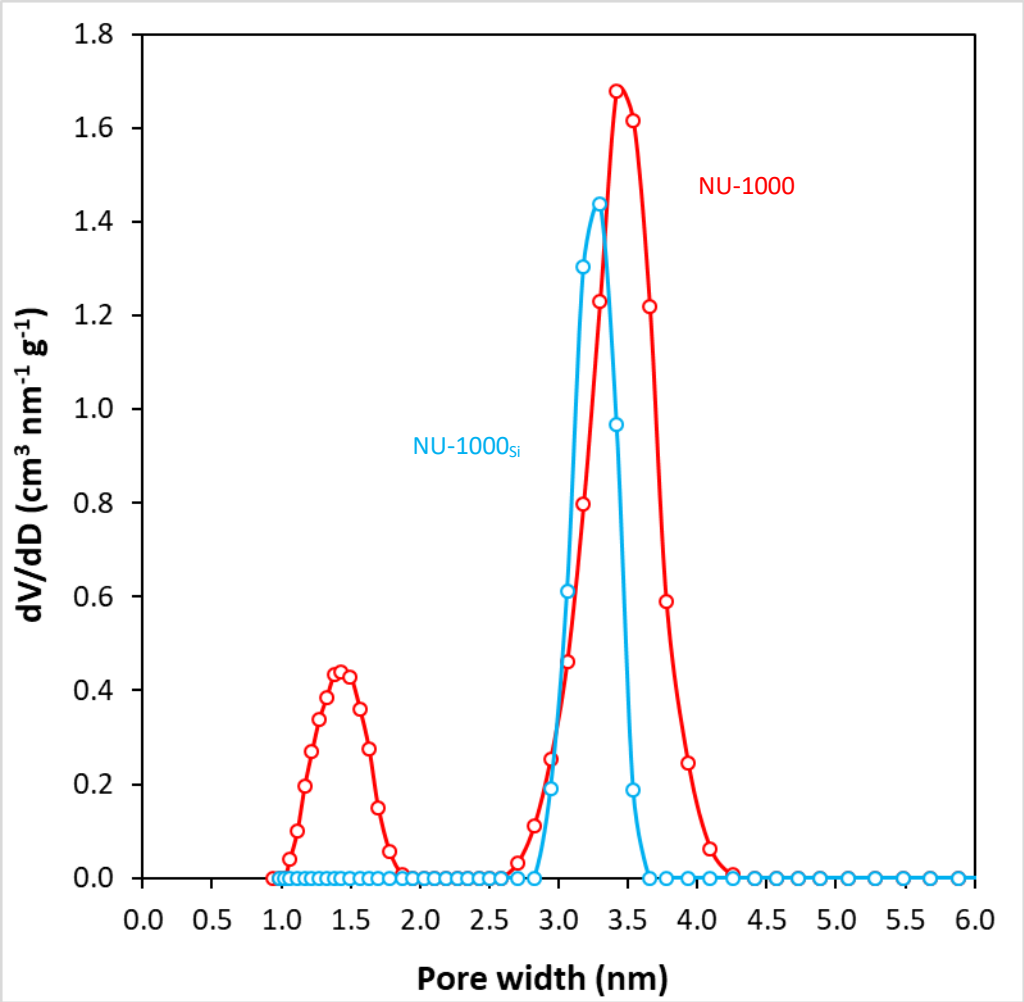

Table S2. Physicochemical data extracted from N_2 physisorption experiments (- 196 °C)

Sample	NLDFT Micropore Volume ($cm^3\ g^{-1}$)	NLDFT Total Pore Volume ($cm^3\ g^{-1}$)	BET Specific Surface Area ($m^2\ g^{-1}$)	NLDFT Mode Pore Sizes (nm)
NU-1000	0.19	1.2	1907	1.4 – 3.4
$NU\text{-}1000_{Si}$	0.00	0.6	916	3.2

Figure S10. Fluorescence spectra of solvent, bromobenzene (BrPh), NU-1000 and NU-1000$_{Si}$.

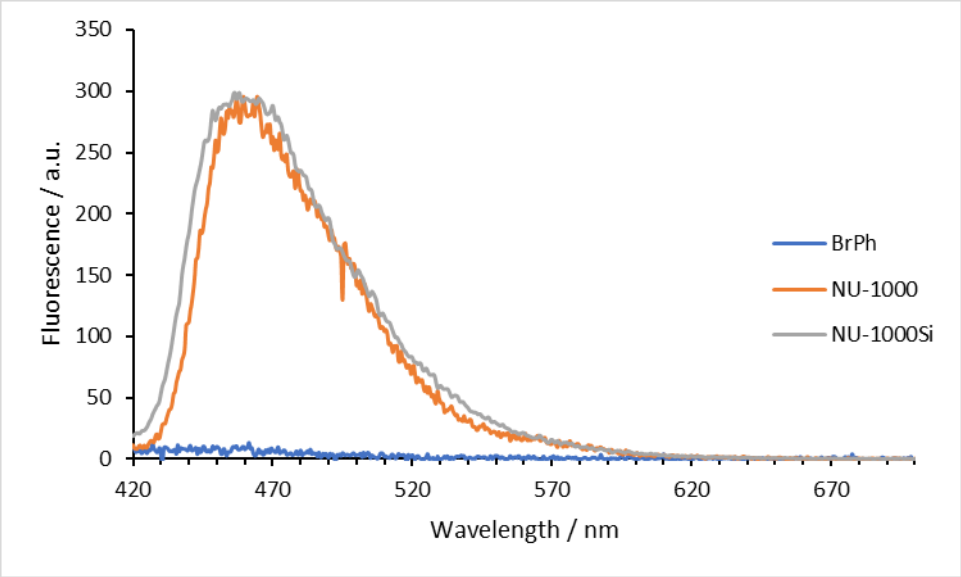

Both NU-1000 and NU-1000$_{Si}$ samples were suspended in bromobenzene.

Figure S11. Thermogravimetric analysis of NU-1000 and NU-1000$_{Si}$.

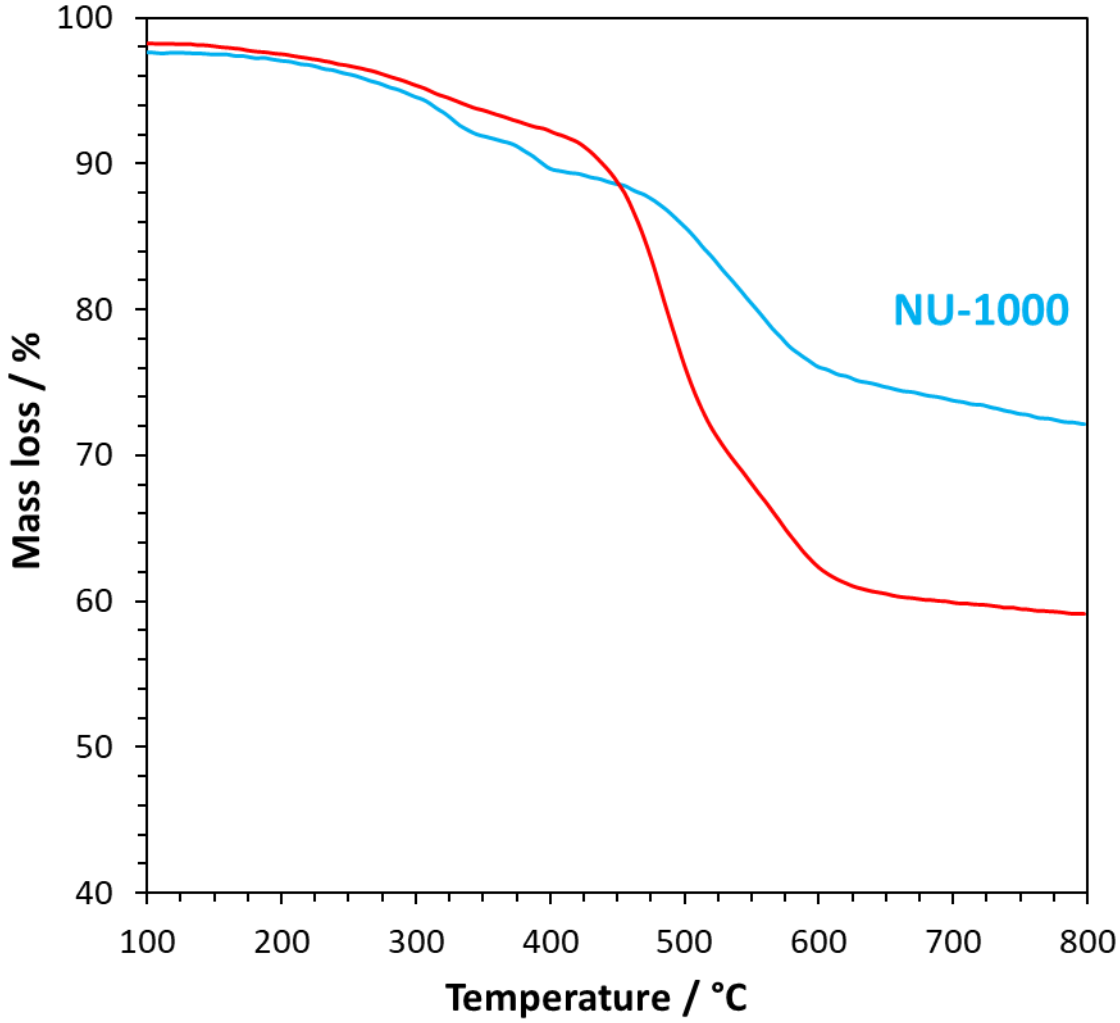

After the isothermal step at 100 °C, NU-1000 shows a weight loss from 97.6% to 72.2% (25.4% loss). NU-1000$_{Si}$ shows a corresponding weight loss from 98.2% to 59.1% (39.1% loss). As NU-1000$_{Si}$ has a higher organic content than NU-1000, the greater percentage mass loss is in accordance to expectations.

References

1. Wang, T. C.; Vermeulen, N. A.; Kim, I. S.; Martinson, A. B. F.; Stoddart, J. F.; Hupp, J. T.; Farha, O. K., Scalable synthesis and post-modification of a mesoporous metal-organic framework called NU-1000. *Nat. Protoc.* **2015,** *11*, 149.
2. Moellmer, J.; Celer, E. B.; Luebke, R.; Cairns, A. J.; Staudt, R.; Eddaoudi, M.; Thommes, M., Insights on Adsorption Characterization of Metal-Organic Frameworks: A Benchmark Study on the Novel soc-MOF. *Microporous Mesoporous Mater.* **2010,** *129*, 345-353.
3. Zhao, W.; Wang, Z.; Malonzo, C. D.; Webber, T. E.; Platero-Prats, A. E.; Sotomayor, F.; Vermeulen, N. A.; Wang, T. C.; Hupp, J. T.; Farha, O. K.; Penn, R. L.; Chapman, K. W.; Thommes, M.; Stein, A., Extending the Compositional Range of Nanocasting in the Oxozirconium Cluster-Based Metal–Organic Framework NU-1000—A Comparative Structural Analysis. *Chem. Mater.* **2018,** *30*, 1301-1315.
4. Deria, P.; Mondloch, J. E.; Tylianakis, E.; Ghosh, P.; Bury, W.; Snurr, R. Q.; Hupp, J. T.; Farha, O. K., Perfluoroalkane Functionalization of NU-1000 via Solvent-Assisted Ligand Incorporation: Synthesis and CO2 Adsorption Studies. *J. Am. Chem. Soc.* **2013,** *135*, 16801-16804.
5. Kongwudthiti, S.; Praserthdam, P.; Tanakulrungsank, W.; Inoue, M., The influence of Si–O–Zr bonds on the crystal-growth inhibition of zirconia prepared by the glycothermal method. *J. Mater. Process. Technol.* **2003,** *136*, 186-189.
6. Launer, P. J.; Arkles, B., Infrared analysis of organosilicon compounds: spectra-structure correlations. In *Silicone Compounds: Silanes and Silicones*, 3rd ed.; Larson, B. A. G. L., Ed. Gelest, Inc.: Morrisville, PA, 2013; pp 175-178.
7. Damaskin, B. B.; Ivanova, R. V., Structure of the Electrical Double Layer in Non-aqueous Solvents. *Russian Chemical Reviews* **1979,** *48*, 932-947.
8. Beunis, F.; Strubbe, F.; Marescaux, M.; Neyts, K.; Verschueren, A. R. M., Diffuse double layer charging in nonpolar liquids. *Appl. Phys. Lett.* **2007,** *91*, 182911.